Temperature dependence of the resistance of a two-dimensional topological insulator in a HgTe quantum well

G. M. Gusev,[1] Z. D. Kvon,[2,3] E. B. Olshanetsky,[2] A. D. Levin,[1] Y. Krupko,[4] J. C. Portal,[4,5,6]
N. N. Mikhailov,[2] and S. A. Dvoretsky[2]

[1]*Instituto de Física da Universidade de São Paulo, 135960-170, São Paulo, SP, Brazil*
[2]*Institute of Semiconductor Physics, Novosibirsk 630090, Russia*
[3]*Novosibirsk State University, Novosibirsk, 630090, Russia*
[4]*LNCMI-CNRS, UPR 3228, BP 166, 38042 Grenoble Cedex 9, France*
[5]*INSA Toulouse, 31077 Toulouse Cedex 4, France*
[6]*Institut Universitaire de France, 75005 Paris, France*

We report resistance measurements in HgTe wells with an inverted band structure near the charge neutrality point (CNP), where the system is expected to be a two-dimensional topological insulator with a dominant edge states contribution. The sample resistance is found to be about 100 times higher than the resistance quantum $h/2e^2$. Surprisingly, instead of a strong temperature dependence expected in such a seemingly insulating state the resistance at the CNP is found to be temperature independent at low temperatures. The experimental results are compared to the recent theoretical models.

I. INTRODUCTION

Two-dimensional (2D) topological insulators (TI) (quantum spin Hall insulators) are characterized by a bulk energy gap and gapless boundary modes that are robust to impurity scattering and electron-electron interactions [1–3]. The 2D quantum spin Hall insulator (QSHI) has been realized in HgTe quantum wells with inverted band structure [4,5]. This system is characterized by an intrinsic spin-orbit interaction, which leads to the formation of helical edge modes with opposite spin polarization counter propagating at a given edge.

The electron conductance of a 2DTI is quantized in units of the universal value $2e^2/h$ as was observed in short and clean micrometer-scale Hall bars [5]. However, the quantized ballistic transport has not been seen in a sample with dimensions above a few microns [4–7]. Understanding why the resistance quantization is difficult to observe in macroscopic samples requires further investigation. An evaluation of the deviation of the conductivity from the quantized value has been performed in several theoretical models. In particular, the combined effect of the weak interaction and disordered scattering in helical Luttinger liquid (LL) channel results in a temperature dependent deviation from $2e^2/h$ which scales with temperature to the power of 4 (Ref. [8]) or 6 (Refs. [9,10]). Another way to understand the observation of resistance exceeding the quantized value is to consider the possible scattering processes at the edge. Classical and quantum magnetic impurities introduce the backscattering between counter propagating channels [11]. Using a somewhat different approach, an edge state transport theory in the presence of spin orbit Rashba coupling has been developed [12].

Recently interaction of the helical states with multiple puddles of charge carriers formed by fluctuations in the donor density has been considered in 2D topological insulators based on HgTe quantum wells [13]. Using scanning gate microscopy, well-localized metallic regions along the edge have been found [14], probably due to potential fluctuations, which might be responsible for scattering between the counterpropagating states. This model also agrees with the observation of mesoscopic fluctuations in resistance with gate voltage, which can be qualitatively explained by the presence of charge puddles in the well [4,5,15].

Despite the existence of a large number of theoretical models and predictions, the temperature dependence of resistance in long 2DTI samples has not yet been systematically studied. In the present paper, we investigate resistance of the 2DTI with a dominant edge state contribution to the transport. The experiment demonstrates a weak temperature dependence of resistance at a level 100 times higher than the quantum unit $2e^2/h$. One of the possible explanations is the fluctuation of the local insulating gap width induced by smooth inhomogeneities, which can be represented as metallic puddles or dots [13].

II. EXPERIMENT

The $Cd_{0.65}Hg_{0.35}Te/HgTe/Cd_{0.65}Hg_{0.35}Te$ quantum wells with (013) surface orientations and width d of 8–8.3 nm were fabricated by molecular beam epitaxy. A detailed description of the sample structure has been given in Refs. [16–18]. Device A is designed for multiterminal measurements, while device B is a six-probe Hall bar. Device A consists of three 4 μm wide consecutive segments of different length (2, 8, 32 μm), and seven voltage probes. Device B was fabricated with lithographic length 6 μm and width 5 μm (Fig. 1, top panel). The ohmic contacts to the two-dimensional gas were formed by the in-burning of indium. To fabricate the gate, a dielectric layer containing 100 nm SiO_2 and 200 nm Si_3Ni_4 was first grown on the structure using the plasmochemical method. Then a TiAu gate with the dimensions 62×8 μm^2 (device A) and 18×10 μm^2 (device B) was deposited. Several devices with the same configuration have been studied. The density variation with the gate voltage is $(1.09 \pm 0.01) \times 10^{15}$ m^{-2} V^{-1}. The electron mobility in these samples is a function of the carrier density with a maximum of the order
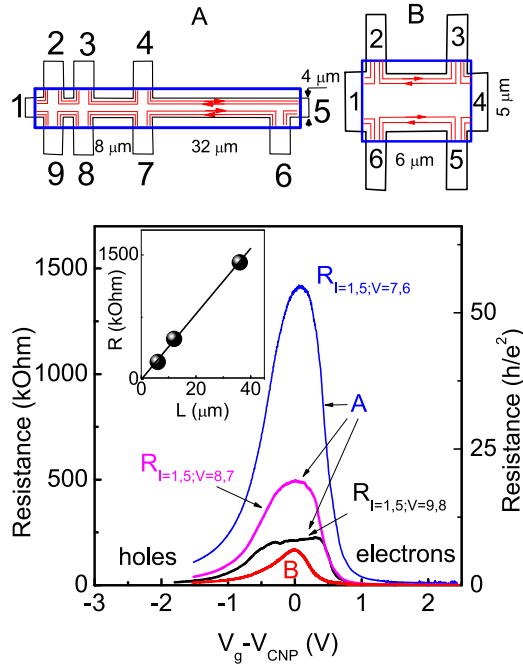
FIG. 1. (Color online) (a) Resistance R_{Local} as a function of gate voltage at zero magnetic field measured between various voltage probes for samples A and B, $T = 4.2$ K, $I = 10^{-9}$ A. The inset shows resistance dependence on the effective distance between probes L. Top panel shows schematic view of the samples. The perimeter of the gate is shown by a blue rectangle.

of $\mu_n = 250 \times 10^3$ cm^{-2}/V s at $n_s = 2 \times 10^{11}$ cm^{-2}, while the hole mobility shows a saturation $\mu_p = 20 \times 10^3$ cm^{-2}/V s for the carrier density above $p_s = 1.5 \times 10^{11}$ cm^{-2}. Transport measurements in the described structures were performed in a variable temperature insert (VTI) cryostat (temperature range 1.4–60 K), in a He$_3$ cryostat (temperature range 0.3–3 K) and in a dilution refrigerator (temperature range 0.05–2 K). We used a standard four point circuit with a 3–13 Hz ac current of 0.1–100 nA flowing through the samples. A typical 100 Mohm resistance connected in series with each sample was used in order to keep the current constant. The carriers' density in HgTe quantum wells can be electrically modified with gate voltage V_g. A typical dependence of the four-terminal R resistances of devices A and B as a function of V_g is shown in Fig. 1. The resistance R of device A corresponds to the configuration where the current flows between contacts 1 and 5 and the voltage is measured between different probes. The measured resistance exhibits a peak that is much greater than the universal value $h/2e^2$, which is expected for the QSHI phase. This value varies linearly with the distance between probes L (see inset). It is worth noting that the contacts to QSHI are assumed to be thermal reservoirs, where the electron states with opposite spins are mixed. In contrast to the quantum Hall effect, where the mixing of the edge states occurs within metallic Ohmic contacts, in our samples this takes place in the 2D electron gas region outside the metallic gate due to a finite bulk conductivity. Therefore, the effective length of the 1D channels L exceeds the distance between the probes of the Hall bar by 3–4 μm. It would be expected that reflection occurs when a 1D electron wave hits the interface

between the ungated part of the sample and the 2DTI regions, which may result in a resistance greater than $h/2e^2$. The linear dependence of resistance on L rules out this possibility and suggests that the high resistance value is more likely the result of backscattering between counter propagating edge channels.

One can see in Fig. 1 that device B shows a smaller and narrower resistance peak. The Hall coefficient (not shown) reverses its sign and $R_{xy} \approx 0$ when R approaches its maximum value [18], which can be identified as corresponding to the charge neutrality point (CNP). The variation of the gate voltage results in a shift of the Fermi level with respect to the energy bands, transforming the quantum wells from a n-type conductor to a p-type conductor via a QSHI state.

Figure 2(a) shows the resistance of device A as a function of inverse temperature. We see that resistance decreases sharply for temperatures above 25 K while saturating below
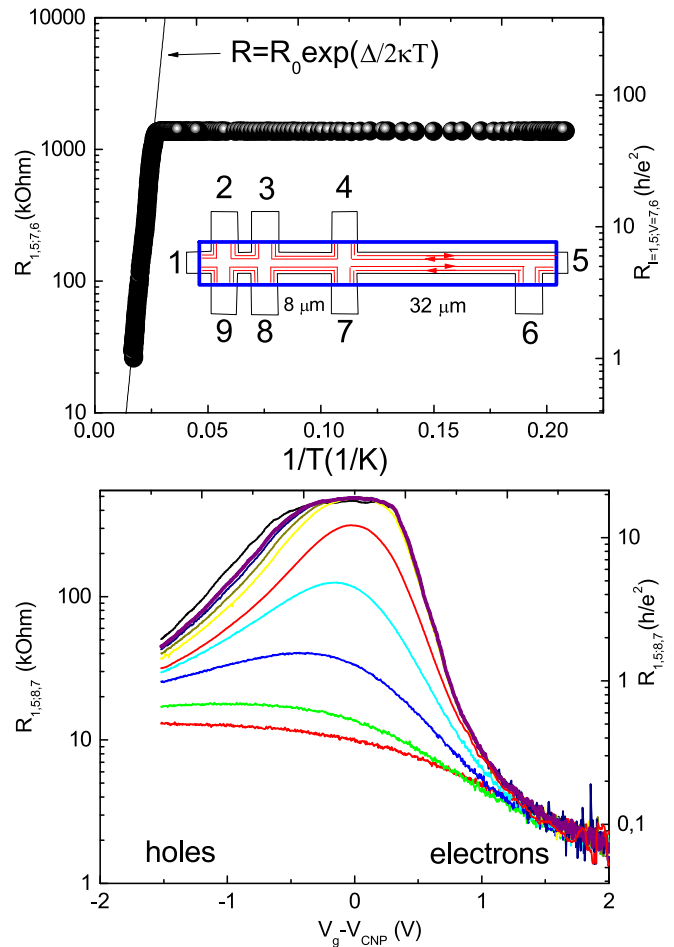

FIG. 2. (Color online) (a) Resistance $R_{1,5;7,6}$ corresponding to the configuration when the current flows between contacts 1 and 5, and the voltage is measured between contacts 7 and 6, as a function of the inverse temperature at the charge neutrality point. The solid line is a fit of the data with the Arrhenius function where $\Delta = 200$ K. The inset shows the schematic view of the sample. (b) Resistance $R_{1,5;8,7}$ ($I = 1, 5; V = 8, 7$) as a function of gate voltage for different temperatures, (T(K): 1.5, 2.5, 3, 3.5, 4.2, 10, 19, 29, 40, 53, 62), $I = 10^{-9}$ A.

20 K. We find that the profile of the $R_{1,5;7,6}$ temperature dependencies above $T > 25$ K fits very well the activation law $\sim\exp(\Delta/2kT)$, where Δ is the activation gap. Figure 2(b) shows the evolution of the resistance-voltage profile with temperature. We see that the electronic part of the dependence is weakly dependent on temperature in the accessible range of temperature, while the hole part shows a strong T dependence with a saturation at low T. The question about the temperature dependence of the resistance outside of CNP in the region with dominant bulk transport requires further detailed theoretical and experimental study, which is out of scope of our paper. The thermally activated behavior of resistance above 25 K corresponds to a gap of 17 meV between the conduction and valence bands in the HgTe well. Recent theoretical calculations based on the effective 6×6 matrix Hamiltonian predicted a gap of $\approx$30 meV for 8 nm HgTe wells with the [013] interface [19]. The mobility gap can be smaller than the energy gap due to disorder. It is worth noting that the disorder parameter, which can reduce the energy gap in QSHI, is related to the deviations of the HgTe quantum well thickness from its average value [20] rather than to the random potential due to charged impurities. The saturation of resistance at low temperature is completely unexpected
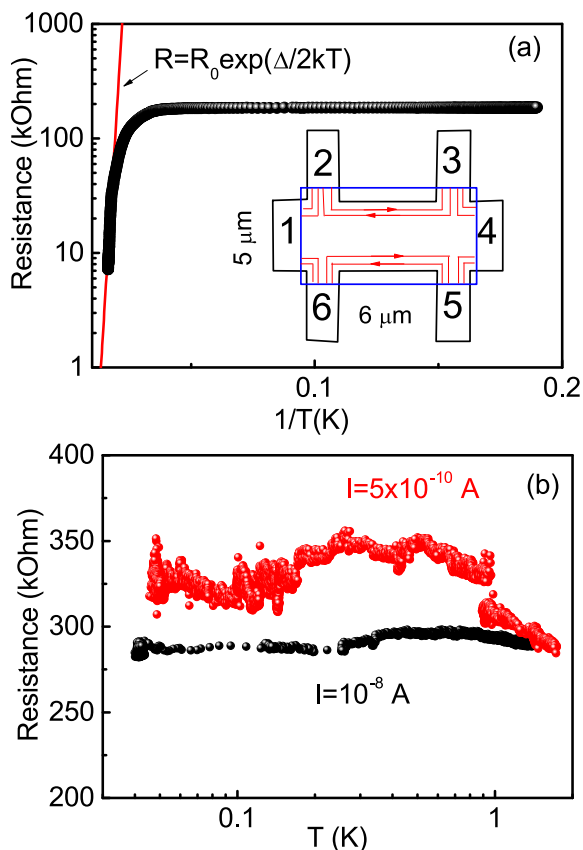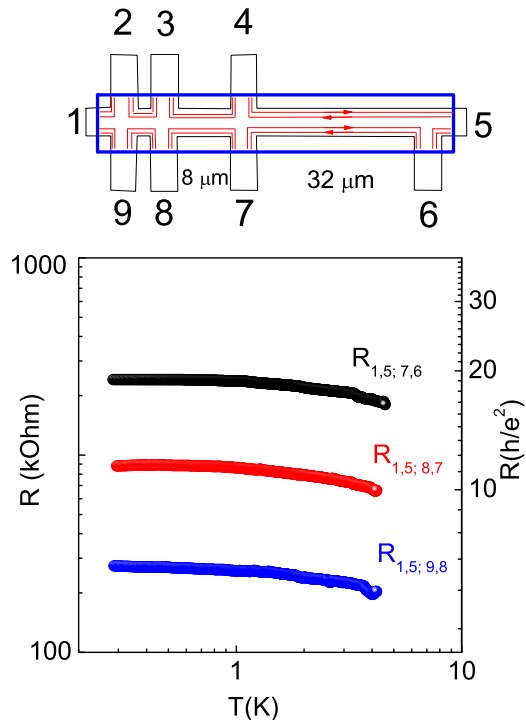

FIG. 4. (Color online) Resistance R of sample A as a function of temperature at the charge neutrality point ($V_g - V_{CNP} = 0$) measured from various voltage probes in the temperature interval 4–0.3 K, $I = 10^{-9}$ A. The top panel shows a schematic view of the sample.

because the electrons are in a supposedly strongly localized regime, where the electrical resistivity of the system is two orders of magnitude greater than the quantum of resistance $h/2e^2$.

Figure 3(a) shows the resistance of device B as a function of inverse temperature. The data above 25 K nicely fits with activation behavior, however, the activation gap is two times larger than in device A. We attribute the larger value of Δ to the better quality of the sample. For example, Fig. 1 shows that the resistivity peak in device B is narrower, and it could be argued that disorder in the sample is considerably smaller. In order to prevent overheating effects by the applied current, we study the current dependence of resistance. The resistance does not change much when the current is varied by three orders of magnitude and preserves the saturation with lowering the temperature both at high and low currents. In Fig. 3(b) we present the T dependence of $R_{1,4;5,6}$ ($I = 1, 4$; $V = 5, 6$) at the CNP for two values of current measured in a wide temperature range 50 mK $< T < 2$ K. We see that for both current levels resistance is constant and does not depend on T.

In Fig. 4 we present the T dependence of resistance in device A. We see that the resistance increases with the temperature decreasing, but there is no significant temperature dependence in the temperature interval 4–0.3 K. This behavior is also inconsistent with what might be expected for Anderson localization, Fermi liquid, or Luttinger liquid models [21].

FIG. 3. (Color online) (a) Resistance $R_{1,4;5,6}$ ($I = 1, 4$; $V = 5, 6$) of sample B as a function of inverse temperature. The solid line is a fit of the data with the Arrhenius function where $\Delta = 400$ K. The inset shows a schematic view of the sample. (b) Resistance $R_{1,4;5,6}$ as a function of temperature at the charge neutrality point ($V_g - V_{CNP} = 0$) for two different current values.

III. DISCUSSION

In the rest of this paper we will focus on several proposed models that can explain the deviation of resistance from the quantized value. The first scenario describes the problem of a single quantum impurity interacting with the helical edge Luttinger liquid state [11]. The spatially inhomogeneous electrostatic potential leads to a bound state which traps odd numbers of electrons and forms magneticlike impurities. For a large Luttinger parameter $K > 1/4$ corresponding to a weak electron-electron interaction, conductance is suppressed at low but finite temperatures and restored to the quantized value again for $T \to 0$. For a strong interaction, which corresponds to a small Luttinger parameter $K < 1/4$, the system becomes a LL insulator and the conductance scales with temperature as $G(T) \propto T^{2(1/4K-1)}$. Note, however, that for the top gated samples, parameter K can be estimated by the expression given in Ref. [22]. In particular, we obtain $K \approx 0.6$, which corresponds to a weak coupling regime.

The second scenario relies on the localization of electrons due to fluctuations of the Rashba spin-orbit interaction caused by charge inhomogeneity in the presence of e-e interactions [12]. The localization length strongly depends on the Luttinger parameter K and can exceed 10 μm for $K > 0.35$. Note, however, that suppression of conductivity due to localization leads to the exponential dependence on temperature. Moreover, the Rashba-induced localization scenario predicts a strong dependence on sample length, which disagrees with our observations.

A third scenario has been recently suggested in Ref. [13], where the inelastic spin flip backscattering within each boundary due to multiple puddles created by the inhomogeneous charge distribution has been considered. The puddles should be small and rare in order to provide a small tunneling probability in the bulk, while on the other hand, few puddles should occur in the vicinity of the edge, allowing for spin dephasing between counterpropagating states. Self-averaging resistance of the sample with edge state dominated contribution to transport is given by [13]:

$$R \sim \frac{h}{e^2} \frac{1}{g^2} n_p \lambda \left(\frac{T}{\delta}\right)^3 L, \qquad (1)$$

where n_p is the density of the puddles, $\lambda = \hbar v/E_g \approx 18$ nm is the electron penetration depth into the puddles ($v \approx 5.5 \times 10^7$ cm/s is the electron velocity, $E_g \simeq 20$ meV is the forbidden gap), g is the dimensionless conductance within the dot (puddle), δ is the mean level spacing within the dot, L is the distance between probes (length of the edge states). Rewriting Eq. (1) in the form $R = \frac{h}{e^2}\rho_0 L$ and comparing it with our results, shown in Fig. 1, we obtain $\rho_0 = 15 \times 10^3$ (e^2/h)/cm = 1.5 $(e^2/h)/\mu$m. This confirms that coherent ballistic transport might occur on the micron length scale. The density of the puddles can only be roughly estimated from the ratio of the total carrier density to the average number of electrons in the puddles. Note that the puddles become populated when the local potential fluctuations exceed half of the forbidden gap. The resulting equations for characteristic donor density n_0 and density of puddles n_p have been obtained in Ref. [13]:

$$n_0 = \frac{E_g^2 \kappa^2}{8\pi e^4 ln\left\{l_g^2/[(2l_g - l_d)l_d]\right\}}, \qquad (2)$$

$$n_p \sim \left(\frac{1}{l_g a_B}\right)\left(\frac{n_d}{n_0}\right) \exp(-n_0/n_d), \qquad (3)$$

where $\kappa = 13$ is the dielectric constant, $l_g \approx 343$ nm is the distance to the gate, $l_d \approx 8$ nm is the distance to the donors, $n_d \sim 2 \times 10^{11}$ cm^2 is the donor density, and $a_B = \frac{2\hbar v}{\alpha E_g}2 \approx 120$ nm ($\alpha = e^2/\kappa\hbar v = 0.3$). From Eqs. (2) and (3), we found $n_0 \approx 4 \times 10^{10}$ cm$^2 \ll n_d$ and $n_p \approx 4 \times 10^9$ cm^2. The dimensionless parameter g can be estimated as $g \sim \sqrt{N} \approx$ 1–2, where N is the number of electrons in the puddle $N \sim a_B n_d^{1/2} \approx$ 2–5. Combining all parameters we finally calculate $\rho_0 = 2 \times 10^3 \left(\frac{T}{\delta}\right)^3 (e^2/h/\text{cm})$ for $g \sim 1$. Energy level spacing is estimated from Coulomb blockade energy in the dot $\delta \sim \alpha^2 E_g \sim$ 1–2 meV. At relatively high temperatures $T \approx 10$ K we obtain $T \sim \delta$ and it is expected that the T dependence is saturated. In this case calculations give a result which is two times smaller than the experimental value (for $g \sim 1$). Note, however, that we don't see any T^3 dependence at temperatures below 10 K in a wide temperature interval (Figs. 3 and 4). In this case we suppose that the energy δ is overestimated, and it is almost two orders of magnitude smaller than is expected from a reasonable size of puddles. Large puddles would yield a large parameter g resulting in a small value of relative resistivity ρ_0. Therefore, our attempts to account for a weak temperature dependence only increase the discrepancy between theory and experiment. However, if a large enough number of puddles are situated at the very edge of the sample, interrupting the edge state current flow, perhaps the resulting temperature dependence would be closer to that observed in this experiment. It is worth noting that condition $n_0 \ll n_d$ corresponds to large puddles separated by p-n junctions and bulk conductivity could shunt the edge state contribution. Observation of large nonlocal resistance indicates that bulk conductivity is suppressed [7]. Further study will be needed to better understand this behavior. In conclusion, we find that, even when the resistance of the HgT quantum wells is two orders of magnitude greater than the resistance quantum $h/2e^2$, implying a strongly localized regime, it is independent of temperature, indicating the absence of an insulating phase. We have attempted to compare these experimental findings with a recent theoretical model [13] where the absence of resistance quantization in a 2DTI is accounted for by tunneling between the edge states and charge carrier puddles in the bulk. We find that while the model gives a satisfactory description of the high resistance value, the explanation of its temperature dependence requires further elaboration of the model.

[1] C. L. Kane and E. J. Mele, Phys. Rev. Lett. **95**, 146802 (2005).

[2] B. A. Bernevig, T. L. Hughes, and S. C. Zhang, Science **314**, 1757 (2006).

[3] J. Maciejko, T. L. Hughes, and S.-C. Zhang, Annu. Rev. Condens. Matter Phys. **2**, 31 (2011).

[4] M. König *et al.*, Science **318**, 766 (2007).

[5] H. Buhmann, Journal. Appl. Phys. **109**, 102409 (2011).

[6] G. M. Gusev, Z. D. Kvon, O. A. Shegai, N. N. Mikhailov, S. A. Dvoretsky, and J. C. Portal, Phys. Rev. B **84**, 121302(R) (2011).

[7] G. M. Gusev, A. D. Levin, Z. D. Kvon, N. N. Mikhailov, and S. A. Dvoretsky, Phys. Rev. Lett. **110**, 076805 (2013); G. M. Gusev, E. B. Olshanetsky, Z. D. Kvon, N. N. Mikhailov, and S. A. Dvoretsky, Phys. Rev. B **87**, 081311(R) (2013).

[8] Thomas L. Schmidt, Stephan Rachel, Felix von Oppen, and Leonid I. Glazman, Phys. Rev. Lett. **108**, 156402 (2012).

[9] Francois Crepin, Jan Car Budich, Fabrizio Dolcini, Patrik Recher, and B. Trauzettel, Phys. Rev. B **86**, 121106(R) (2012).

[10] C. Wu, B. A. Bernevig, and S. C. Zhang, Phys. Rev. Lett. **96**, 106401 (2006).

[11] J. Maciejko, C. X. Liu, Y. Oreg, X. L. Qi, C. Wu, and S. C. Zhang, Phys. Rev. Lett. **102**, 256803 (2009).

[12] A. Ström, H. Johannesson, and G. I. Japaridze, Phys. Rev. Lett. **104**, 256804 (2010).

[13] J. I. Vayrynen, M. Goldstein, and L. I. Glazman, Phys. Rev. Lett. **110**, 216402 (2013).

[14] M. König, M. Baenninger, A. G. F. Garcia, N. Harjee, B. L. Pruitt, C. Ames, P. Leubner, C. Brüne, H. Buhmann, L. W. Molenkamp, and D. Goldhaber-Gordon, Phys. Rev. X **3**, 021003 (2013).

[15] G. Grabecki, J. Wróbel, M. Czapkiewicz, Ł. Cywiński, S. Gierałtowska, E. Guziewicz, M. Zholudev, V. Gavrilenko, N. N. Mikhailov, S. A. Dvoretski, F. Teppe, W. Knap, and T. Dietl, Phys. Rev. B **88**, 165309 (2013).

[16] Z. D. Kvon, E. B. Olshanetsky, D. A. Kozlov, N. N. Mikhailov, and S. A. Dvoretskii, Pis'ma Zh. Eksp. Teor. Fiz. **87**, 588 (2008) [JETP Lett. **87**, 502 (2008)].

[17] E. B. Olshanetsky, Z. D. Kvon, N. N. Mikhailov, E. G. Novik, I. O. Parm, and S. A. Dvoretsky, Solid State Commun. **152**, 265 (2012).

[18] G. M. Gusev, E. B. Olshanetsky, Z. D. Kvon, N. N. Mikhailov, S. A. Dvoretsky, and J. C. Portal, Phys. Rev. Lett. **104**, 166401 (2010); G. M. Gusev, E. B. Olshanetsky, Z. D. Kvon, A. D. Levin, N. N. Mikhailov, and S. A. Dvoretsky, *ibid.* **108**, 226804 (2012).

[19] O. E. Raichev, Phys. Rev. B **85**, 045310 (2012).

[20] G. Tkachov, C. Thienel, V. Pinneker, B. Buttner, C. Brune, H. Buhmann, L. W. Molenkamp, and E. M. Hankiewicz, Phys. Rev. Lett. **106**, 076802 (2011).

[21] I. V. Gornyi, A. D. Mirlin, and D. G. Polyakov, Phys. Rev. Lett. **95**, 206603 (2005); Phys. Rev. B **75**, 085421 (2007).

[22] C. L. Kane and M. P. A. Fisher, Phys. Rev. B **46**, 15233 (1992); Phys. Rev. Lett. **68**, 1220 (1992).